Article

Frustration and the Kinetic Repartitioning Mechanism of Substrate Inhibition in Enzyme Catalysis

Published as part of The Journal of Physical Chemistry virtual special issue "Jose Onuchic Festschrift".

Yangyang Zhang, Mingchen Chen, Jiajun Lu, Wenfei Li,* Peter G. Wolynes,* and Wei Wang*

Read Online

ACCESS | Metrics & More | Article Recommendations | SI Supporting Information

ABSTRACT: Substrate inhibition, whereby enzymatic activity decreases with excess substrate after reaching a maximum turnover rate, is among the most elusive phenomena in enzymatic catalysis. Here, based on a dynamic energy landscape model, we investigate the underlying mechanism by performing molecular simulations and frustration analysis for a model enzyme adenylate kinase (AdK), which catalyzes the phosphoryl transfer reaction ATP + AMP $\leftrightharpoons$ ADP + ADP. Intriguingly, these reveal a kinetic repartitioning mechanism of substrate inhibition, whereby excess substrate AMP suppresses the population of an energetically frustrated, but kinetically activated, catalytic pathway going through a substrate (ATP)-product (ADP) cobound complex with steric incompatibility. Such a frustrated pathway plays a crucial role in facilitating the bottleneck product ADP release, and its suppression by excess substrate AMP leads to a slow down of product release and overall turnover. The simulation results directly demonstrate that substrate inhibition arises from the rate-limiting product-release step, instead of the steps for populating the catalytically competent complex as often suggested in previous works. Furthermore, there is a tight interplay between the enzyme conformational equilibrium and the extent of substrate inhibition. Mutations biasing to more closed conformations tend to enhance substrate inhibition. We also characterized the key features of single-molecule enzyme kinetics with substrate inhibition effect. We propose that the above molecular mechanism of substrate inhibition may be relevant to other multisubstrate enzymes in which product release is the bottleneck step.
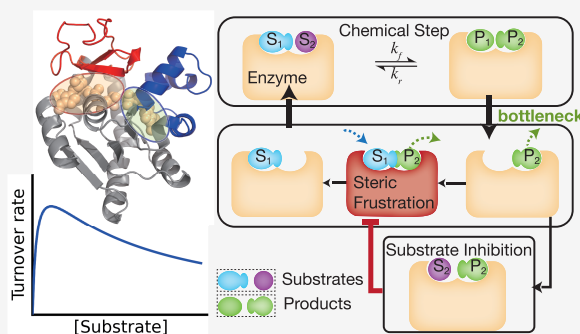
INTRODUCTION

As biomolecular machines, enzymes function via enzymatic cycles, including not only chemical reaction steps, but also substrate-binding and product-release steps, which especially are facilitated by conformational motions.[1] Enzyme kinetics can often be described by the classical Michaelis−Menten equation, which predicts that the turnover rate increases with substrate concentration, but saturates after reaching a maximum value. Many enzymes however show substrate inhibition effects by which the turnover slows down when there is an excess supply of substrate, instead of saturating.[2−14] The substrate inhibition effect at high substrate concentrations is biologically relevant and essential for cell survival.[15] Natural enzymes generally have evolved to minimize substrate inhibition at physiological substrate concentrations.[16]

As one of the most intriguing and counterintuitive observations in enzyme catalysis, the molecular mechanisms of substrate inhibition are still under debate. Excessive substrate may produce unproductive enzyme−substrate complexes by competitively binding to the active site,[3,4,17] thus leading to lowered turnover rate. Another possible mechanism is that the substrate at high concentration may also nonspecifically bind to an alternative site and slow down the population of catalytically competent state through allosteric coupling.[7,18] A general feature for these mechanisms is that the substrate inhibition arises either from the substrate binding step or from the conformational preorganization step required for chemical reactions, which were often described by the competitive or noncompetitive inhibition models traditionally developed for the inhibitor coupled enzyme catalysis.[1] Recent experimental studies also have suggested that substrate inhibition may arise as a secondary effect in which substrate binding to the peripheral site leads to blockade of the product dissociation channel, therefore slowing down the catalysis.[6,19,20] All these previous works provided unprecedented understanding of the substrate inhibition effect by combining bulk-level kinetic measurements, mutation analysis, and kinetic models. Direct observation of the individual key molecular
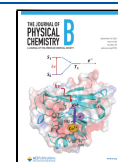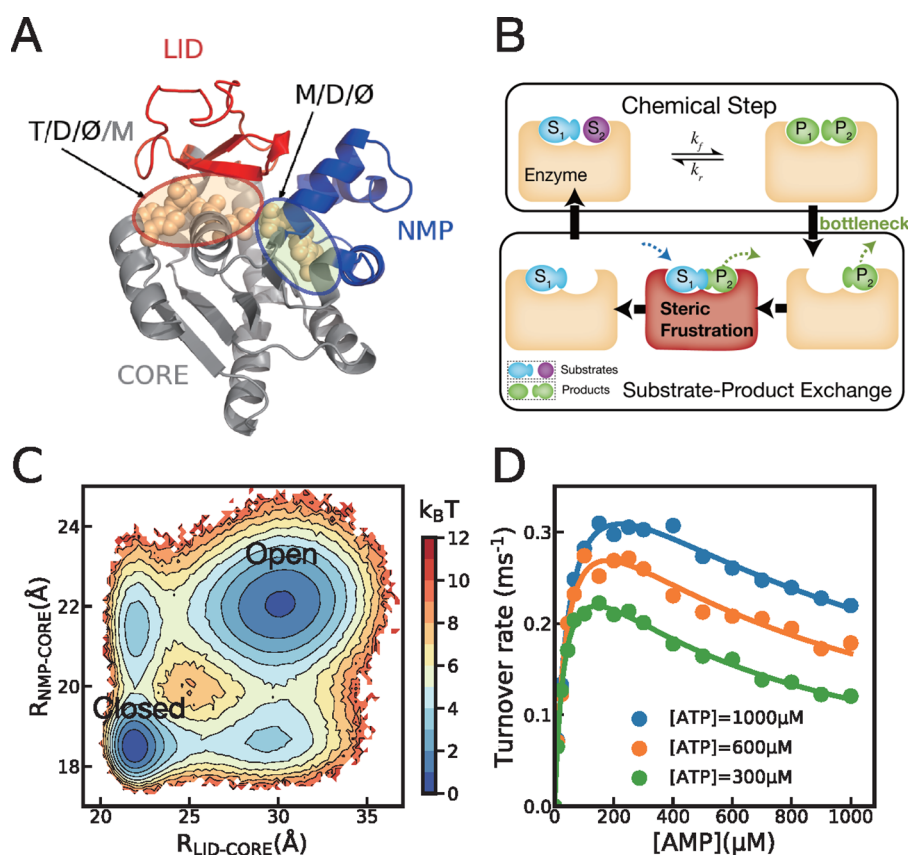
Figure 1. (A) Three-dimensional structure of AdK at the closed state. The three domains are shown by different colors (red, LID; blue, NMP; gray, CORE). The ATP binding site and AMP binding site were labeled by red and blue circles. The binding states of the site with ATP, AMP, ADP, or empty are represented by T, M, D, or ø, respectively. Due to geometrical compatibility, AMP may also nonspecifically bind to the ATP binding site. (B) Schematic diagram showing the sterically frustrated catalytic pathway utilized by the multisubstrate enzyme to overcome the bottleneck product release step. Other parallel pathways with minor distributions have not been shown for clarify. (C) Two-dimensional free energy profile using the distances between the LID-CORE domains and between the NMP-CORE domains as collective coordinates for the wild-type AdK. (D) Turnover rates of the AdK as a function of AMP concentrations with the ATP concentrations being fixed at 300 μM (green), 600 (orange) and 1000 (blue). The solid lines are found by fitting using eq 2.

events involved in substrate inhibition is extremely challenging, since that requires single-molecule characterization of a highly coordinated process involving tight interplay among many individual physical and chemical steps. In this work, we study the molecular mechanism of the substrate-inhibition using a single-molecule level computational model focusing on adenylate kinase (AdK) as a model enzyme.[21]

Adenylate kinase, which catalyzes reversible conversion from ATP and AMP to two ADP molecules, plays a crucial role in energy balance within the cell. It has been widely used as a model system to study the interplay between conformational motions and catalysis.[22−31] It has three domains, including the CORE domain, LID domain (ATP binding site), and NMP domain (AMP binding site; Figure 1A).[21] Each of the two binding sites can bind a substrate, a product, or remain empty, leading to nine possible functional binding states (hereafter termed "chemical states"). Experimentally, NMR spectroscopy and single molecule techniques have directly revealed large-scale conformational motions between the open conformation and closed conformation in the absence of substrates.[22,23,32,33] Binding of substrates induces further stabilization of the catalytically competent closed conformations, in which the chemical reaction occurs. Particularly, it has been shown that product release, which is accompanied by conformational fluctuations, is the rate-limiting step of the catalytic cycle.[22,23]

Previous work revealed that multisubstrate enzymes can utilize steric frustration to facilitate the rate-limiting step of enzymatic cycle using AdK as a model system.[31,34] In this mechanism, the substrate for the next catalytic round binds before the release of the bottleneck product at the neighboring site, thereby forming a substrate-product cobound complex with steric frustration. The product can then be actively squeezed out using the driving energy from substrate binding (Figure 1B and Supporting Information, Figure S1). For the enzyme AdK, the substrate inhibition at high AMP concentrations has been demonstrated experimentally in several previous works,[13,16,17,35] but the underlying mechanism is in debate.

In this paper, by performing molecular dynamics simulations of the whole enzymatic cycle of the AdK with a dynamic energy landscape model buttressed by available experimental data,[31] we study substrate inhibition at the single-molecule level. The simulations not only directly reveal the tight interplay among the individual physical and chemical steps involved in the cycle, but also uncover a "kinetic repartioning" mechanism of the substrate inhibition in which nonspecific binding of excess AMP inhibits the turnover rate by suppressing the population of the energetically frustrated, but kinetically favorable, pathway of the enzymatic cycle. Furthermore, the results illustrate the general relationship between substrate inhibition, the frustration of the energy

landscape, and enzyme conformational equilibrium. The key features of single-molecule level enzymatic kinetics with substrate inhibition are also discussed. This picture is also supported by the results of an energetic survey using the atomistic frustratometer to analyze the various species.[36]

MATERIALS AND METHODS

Dynamic Energy Landscape Model of Single-Molecule Enzymatic Catalysis. The enzymatic cycle is described by a dynamic energy landscape model developed in our previous work.[31] For the AdK with two substrate binding sites, the energy function at a given ligand binding state (ls_1, ls_2) can be written as

$$V(\vec{x}, ls_1, ls_2) = V_{apo}(\vec{x}) + \sum_{i=1,2} V_{bind}^i(\vec{x}, ls_i) \qquad (1)$$

Here ls_1 and ls_2 represent the binding state of the LID domain (ls_1 = T, D, M, or ∅) and NMP domain (ls_2 = M, D, or ∅), respectively. $\vec{x}$ collectively represents the coordinates of the coarse-grained residues at a given structure. $V_{apo}(\vec{x})$ is the structure-based energy function of the enzyme at apo state, which has a double basin topography characterizing the conformational equilibrium between the open and closed conformations.[37−39] $V_{bind}^i(\vec{x}, ls_i)$ is the ligand binding energy of the binding pocket i with binding state ls_i, which leads to different overall energy landscapes dictating the conformational motions of the enzyme at different chemical states.[40] The enzymatic cycle is described as the hopping of the system between energy landscapes and the conformational motions along the corresponding energy landscapes. Both the chemical reaction and the binding/dissociation of the substrate and product, which were realized by a Metropolis Monte Carlo scheme, can change the chemical states, leading to hopping between energy landscapes. Therefore, the underlying assumption of the above dynamic energy landscape model is that the transition path time for the ligand binding/ dissociation is much shorter than the time scale of the protein conformational dynamics, so that we can simulate the ligand exchange as a one-step stochastic process. The chemical reaction is possible only when the enzyme arrives at the catalytically competent state, at which both substrates are bound to the binding sites and the active sites were well preorganized into the native-like closed structure. More details of the dynamic energy landscape model can be found in the Supporting Information and ref 31.

Molecular Simulations and Kinetic Analysis. The simulations were performed using a modified version of Cafemol Package.[41] The PDB structures with the entries 4ake[21] and 1ake[42] were used as the reference structures in constructing the structure-based energy functions for the open and closed states, respectively. The temperature was controlled at 300 K by Langevin thermostat with friction coefficient $\gamma = 0.25\tau^{-1}$ and time step of 0.1τ. Here τ is the reduced time unit in CafeMol. For the calculation of the turnover rate, 20 independent trajectories with the length of 2×10^8 MD steps were simulated for each case. In all the simulations, the concentration of the free ADP was set as zero. As the time unit of the coarse-grained model cannot be directly compared with the laboratory time scales due to the simplification of the degrees of freedom and the energy functions, we have calibrated the time scale of the coarse-grained simulations by mapping the simulated rates of the conformational motions of

the AdK at the apo state to the experimental values. The simulation length of 2×10^8 MD steps can be roughly mapped to 112 ms.[31]

Based on the calculated turnover rate at a fixed ATP concentration and various AMP concentrations, we can extract the important parameters, including the maximal catalytic velocity k_{cat}, Michaelis constant K_M, and the inhibition constant K_I by fitting the data with the following equation.[16]

$$v_0 = \frac{k_{cat}[AMP]}{K_M + [AMP]\left(1 + \frac{[AMP]}{K_I}\right)} \qquad (2)$$

Here K_I can be used to quantify the extent of substrate inhibition.

The frustration analysis was performed by the atomistic frustratometer developed in recent work.[36] The residue– residue (residue–ligand) contacts with frustration index lower than −2.5 (−1.5) are considered as minimally frustrated. Similarly, the contacts with frustration index higher than 0.5 are considered as highly frustrated. The all-atom MD simulations were conducted using Gromacs2021 with AMBER ff14SB force field and TIP3P water.[43−45] A total of 30 independent MD simulations with lengths of 40 ns were conducted to relax the enzyme structures at the temperature of 300 K and pressure of 1.0 atm starting from the native structure for each of the chemical states TD, DD, and MD. The snapshots from the last 10 ns were used for the calculations of the energetic and structural features. Because it is not straightforward to decompose solvent effects into pairwise contact free energies by using the AMBER force field with explicit water, we used the Rosetta energy function to calculate the pairwise contact free energies for the snapshots generated by the atomistic MD simulations. More details of the model and analysis can be found in the Supporting Information.

Calculation of the Mean First Passage Time. In order to characterize the contributions of the component steps of the enzymatic cycle to the substrate inhibition, we calculated the mean first passage time (MFPT) for the product release step and the MFPT for populating the catalytically competent state. The MFPT for the product release was calculated based on the time span for the release of the rate-limiting product ADP. In the calculations of the MFPT for populating the catalytically competent state, the initial state was set as the open conformation without ligand binding, and the final state was set as the TM state with the two domains closed. We performed 400 independent MD simulations with the length of 1×10^7 MD steps starting from the above initial state for each case and calculated the MFPT based on a maximum likelihood estimation method.

RESULTS AND DISCUSSION

Molecular Simulations of Substrate Inhibition with Dynamic Energy Landscape Model. In the dynamic energy landscape model of enzyme catalysis, the enzymatic cycle is envisioned as involving hopping between the energy land- scapes at the different chemical states due to ligand exchange/ chemical reaction and the conformational motions dictated by the corresponding intrinsic energy landscapes.[31] The related model parameters were optimized to reproduce the relative stability of the open and closed conformational states and the ligand binding affinities measured experimentally (see
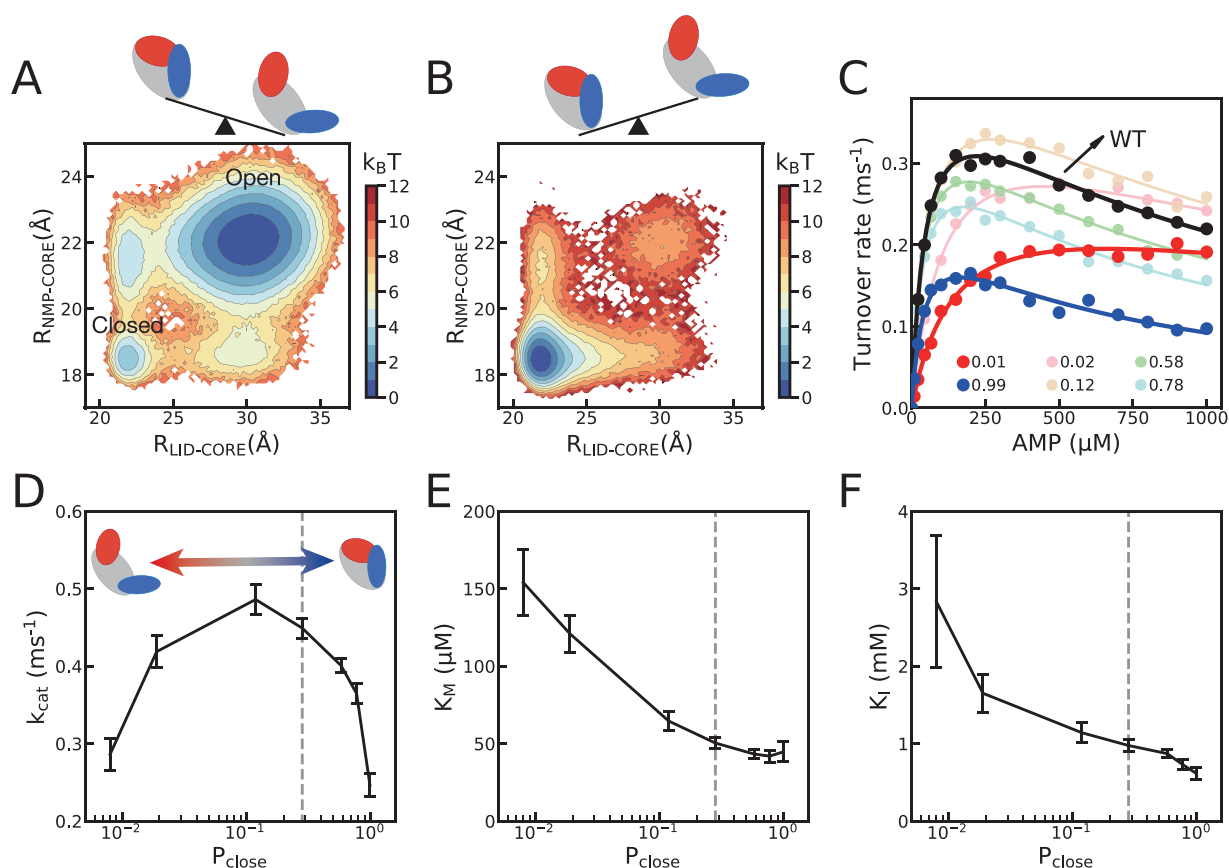
Figure 2. Dependence of the substrate inhibition on the pre-existing protein conformational equilibrium. (A, B) Two-dimensional free energy profiles for enzyme models with extremely open (A, $P_{close} \approx 0.01$) and extremely closed (B, $P_{close} \approx 0.99$) conformational equilibria. The conformational equilibria was tuned by changing the parameters in the dynamic energy landscape model. (C) Turnover rates as a function of AMP concentrations for the enzyme models with different P_{close} values. The solid lines are the fitting by eq 2. The P_{close} values were shown in the panel. (D–F) The enzymatic parameters k_{cat}, K_M, and K_I as a function of P_{close} values. The dash line corresponds to the parameters of the wild-type enzyme.

Supporting Information for details.). The two-dimensional free energy landscape along the reaction coordinates describing the opening and closing motions of the LID and NMP domains shows that the wild type enzyme can sample wide range of conformational space, and both the open and closed conformations have significant populations in the apo state (Figure 1C and Supporting Information, Figure S2). By simulating the whole enzymatic cycle with molecular dynamics, we can calculate the enzyme kinetics at the ensemble level and single-molecule level. Figure 1D shows the turnover rate as a function of the AMP concentration with the ATP concentration being fixed at 300, 600, and 1000 μM. For all these cases, one can observe an initially increasing phase at low AMP concentration range and a decreasing phase at high AMP concentrations, demonstrating typical substrate inhibition effect (Figure 1D). The above results suggest that the dynamic energy landscape model can be successfully used to describe the substrate inhibition effect observed in experiments,[16,35] which makes it possible to investigate the underlying molecular mechanism.

Effects of Pre-Existing Conformational Equilibria on the Substrate Inhibition Effect. The conformational equilibrium in absence of ligands is an intrinsic feature of enzymes. Previous studies for AdK shows that population shift toward the closed conformation induced by mutations tends to slow catalysis.[31,46] In the above discussion, the relative populations of the enzyme conformations were restrained based on available experimental data of the wild-type AdK.[22] To investigate how the conformational equilibrium contributes to substrate inhibition, we tuned the global parameters controlling the relative stability between open and closed conformations in the energy function of the dynamic energy landscape model. In this way we can approximately model the effects of population shifting mutations (see Supporting Information for details.). The resulting models cover a wide range of conformational equilibrium constants, varying from favoring highly open conformations to highly closed conformations (Figure 2A,B and Supporting Information, Figure S3). By performing molecular dynamics simulations of the enzymatic cycle at various AMP concentrations, we have calculated the turnover rates for these enzyme models. Strikingly, the kinetic profiles for the above enzyme models show dramatic differences. For the enzyme models favoring highly open conformations, the turnover rates show classical Michaelis–Menten behavior, as featured by the saturation of the rate at the maximum value with the increasing of AMP concentration. These lack then a substrate inhibition effect (Figure 2C, red). In comparison, for the enzyme models that have a significant population of closed conformation, the substrate inhibition effect can be clearly observed (Figure 2C, blue and black).
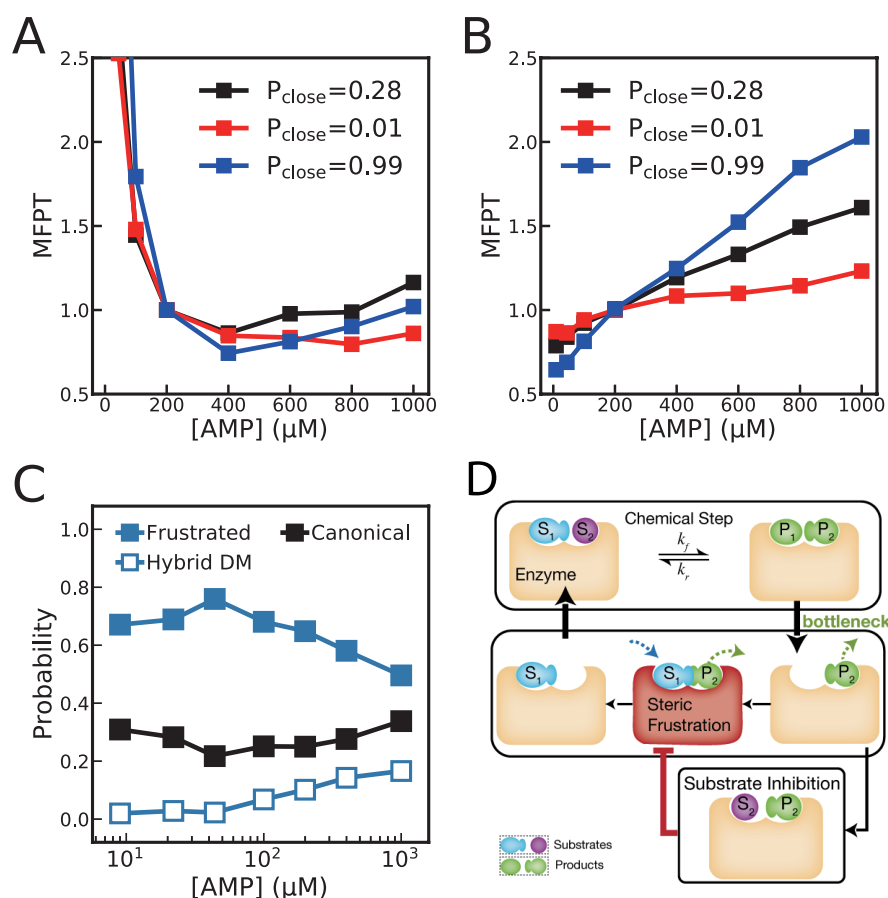
Figure 3. Kinetic repartitioning mechanism of substrate inhibition. (A) Mean first passage time (MFPT) for sampling the catalytically competent complex (including productive substrate binding and conformational closing steps) as a function of AMP concentrations for the ADK models with different P_{close}. The MFPT was normalized by the value at the AMP concentration of 200 μM. (B) MFPT of product release as a function of AMP concentrations for the ADK models with different P_{close}. (C) Probabilities of the frustrated pathway (blue), canonical pathway via empty state (black), and other pathways via nonfrustrated substrate–product cobound state (DM) as a function of AMP concentrations. The ATP concentration was fixed at 1000 μM in all the above simulations. In this work, chemical state "XY" represents that the LID domain site and NMP domain site are occupied by "X" and "Y", respectively, with X = T, D, M, or ∅ and Y = M, D, or ∅. For example, the chemical state TD (DM) represents the chemical state in which the LID domain site and NMP domain site are occupied by ATP and ADP (ADP and AMP), respectively. (D) Schematic showing the substrate inhibition mechanism, whereby nonspecific binding of excess substrate S_2 to the S_1 site suppresses the population of the frustrated catalytic pathway and, therefore, the overall turnover rate. Other competitive pathways with increased probabilities at excess substrate were not shown here for clarity.

To more quantitatively characterize the effect of the conformational equilibria, we fitted the turnover rate profiles using eq 2 and extracted the key kinetic parameters, including the maximal catalytic velocity k_{cat}, Michaelis constant K_M, and inhibition constant K_I (Materials and Methods). The values of the fitting kinetic parameters are then plotted as a function of the populations of the closed conformation (P_{close}, which was used to characterize the pre-existing conformational equilibrium) in Figure 2D−F. One can see that the maximal catalytic rate changes with the P_{close} nonmonotonically. Either extremely open or closed conformational equilibria tend to slow down enzymatic catalysis (Figure 2D). More detailed analysis shows that with the increasing of P_{close}, the bottleneck product release becomes more difficult, which leads to a decreased maximal catalytic rate (Supporting Information, Figure S4). On the contrary, when the conformational equilibrium is highly biased to the open conformation, the productive substrate binding and the conformational preorganization to the catalytically competent state become more difficult, which also tends to slow down the turnover rate. The Michaelis constant K_M decreases with P_{close} as also observed in previous experimental

measurement.[46] This is easy to understand because more closed conformations often lead to increased substrate binding affinity (Figure 2E). Strikingly, the K_I values monotonically decrease with the increasing of the P_{close} (Figure 2F). Such results clearly demonstrated that there is a tight interplay between the enzyme conformational equilibrium and the extent of substrate inhibition. Enzymes with the conformational equilibrium biased to more closed conformations tend to show stronger substrate inhibition effect. Interestingly, previous experimental work by Adkar and co-workers showed that the substrate inhibition is strongly correlated with protein stability.[16] Higher stability tends to cause stronger inhibition. Experimental work has also shown that the AdK mutants with higher stability tend to bind substrate more tightly.[16] Because the closed conformation of AdK has a higher affinity for substrate binding,[47] the experimental results suggest that the mutations increasing the overall enzyme stability also stabilize the closed conformation. Therefore, the relation between the substrate inhibition and the pre-existing conformational equilibria revealed in this work is in line with previous

experimental observations on the relation between substrate inhibition and protein stability of AdK.[16]

In the experimental work by Adkar et al., protein stability was tuned by single-point mutations.[16] In contrast, in the above simulations, the global energy gap parameters controlling the conformational equilibrium were tuned to model the mutation effects. To more closely compare the simulation results and the experimental data, we have also introduced single-site mutations to the protein AdK by modifying the interaction strengths between the mutated site and all other neighboring residues. Similar results were obtained (Supporting Information, Figures S5 and S6).

Kinetic Repartitioning Mechanism of Substrate Inhibition and Suppressed Frustration. The single-molecule level enzyme model allows an in depth characterization of the individual steps and their interplay, so as to understand the underlying mechanism of the substrate inhibition. To this end, we calculated the mean first passage time (MFPT) for the enzyme to arrive at the catalytically competent state, which involves the productive substrate binding and conformational preorganization steps, starting from the fully open conformation with the active sites unoccupied. We also calculated the MFPT for the release of the (bottleneck) product ADP starting from the DD state with the two domains closed. One can see that the time needed for populating the catalytically competent state is insensitive to the AMP concentrations at the high concentration range (Figure 3A). Even for the enzyme models with extremely open conformational equilibrium for which sampling the catalytically competent complex is the rate-limiting event, increasing the AMP concentration does not affect the MFPT at high concentration range. On the contrary, the time needed for the product release has a strong dependence on the AMP concentration. With the increasing of the AMP concentrations, the product release becomes slower, particularly for enzymes with larger P_{close} values (Figure 3B). Such features clearly suggest that the substrate inhibition for AdK dominantly arises from the product release step, instead of the steps involved in the population of the catalytically competent complex, as has usually been proposed in previous works for the AdK based on bulk experiments.[13,35] The above results demonstrate the importance of examining dynamics at the single-molecule level in characterizing the mechanism of the substrate inhibition effect.

As discussed in previous work, the enzymatic cycle of the multisubstrate enzyme AdK involves multiple pathways.[31] In addition to the canonical pathway in which substrate binding occurs after the full release of the two product ADP molecules, an energetically frustrated, but kinetically activated, pathway was dominantly populated (Figure 1B and Supporting Information, Figure S1). In this frustrated pathway, new substrate ATP binds before the dissociation of the bottleneck product ADP at the neighboring site (NMP domain site), leading to a substrate (ATP)−product (ADP) cobound complex in which the binding pockets are frustrated due to steric incompatibility.[31,34] Such steric frustration enables an active mechanism of product release driven by substrate-binding energy, facilitating the enzymatic cycle. Consequently, the catalytic cycle with the frustrated pathway contributes to the accelerated catalysis. We calculated the probabilities of different pathways at different AMP concentrations. One can see that with increasing AMP concentrations, the frustrated pathway contribution decreases (Figure 3C), which is

accompanied by an increased occupation of the LID domain site by excess AMP (Supporting Information, Figure S7). In contrast, the probabilities of other slow pathways, including the canonical pathway via the apo state and the pathway via the nonfrustrated ADP-AMP cobound state, increase with the AMP concentrations. As the frustrated pathway represents the kinetically favorable pathway, suppressing this pathway naturally causes decreased turnover. These results strongly suggest that the observed substrate inhibition effect of the AdK results from the decreased population of the frustrated pathway at high AMP concentration, suggesting a kinetic repartitioning mechanism for the substrate inhibition effect (Figure 3D and Supporting Information, Figure S8). Here we use the term "repartitioning" to emphasize the suppression of the kinetically favorable pathway by the nonspecific binding of excess substrate AMP. Such a mechanism is consistent with the observation that substrate inhibition arises from the bottleneck product release step. The interplay between the suppressed population of frustrated pathway and the substrate inhibition can also be illustrated by both the relaxation dynamics and steady distribution of the different chemical states based on Markov state model analysis (Supporting Information, Text and Figure S9).

In line with the above results, recent experimental work on a mutant of haloalkane dehalogenase suggested that substrate inhibition can arise from the product release step.[19,20] Different from the AdK situation, the slow down of product release was considered to be the result of steric blockage in the product dissociation channel due to substrate binding to a peripheral site, which is different from the kinetic repartitioning mechanism observed in this work. In addition, the kinetic repartitioning mechanism is also consistent with the experimental observation that there is no sign of substrate ATP inhibition for AdK,[46,48] because a high concentration of ATP does not suppress the population of the frustrated pathway.

Characterizing the Localized Frustration by Atomistic Frustratometer. Previous work based on statistical surveys of structural databases and energetic analysis have demonstrated the crucial role of local frustration on the biological functions of proteins.[36,49,50] It was shown that AdK at the closed conformation has a more extensive minimally frustrated network of contacts that rigidifies the enzyme.[51] In addition, the hinge regions tend to be highly frustrated, which favors the rigid-body motions of the LID and NMP domains involved in the conformational transitions between the open and closed forms.[51] Recent development of the atomistic frustratometer allows a quantitative characterization of frustration for ligand binding.[36] Using this computational tool, we calculated the frustration index for the binding sites of the two product ADPs at the chemical state DD (Figure 4 and Supporting Information, Text.).[36] One can see that the frustration index for the ADP binding at the NMP domain site is much smaller than that for ADP binding at the LID domain site, as measured by the higher number of minimally frustrated contacts between the NMP domain ADP and its binding residues (Figure 4A, green lines; Supporting Information, Figure S10). These results suggest that the product ADP can fit more optimally to the binding site at the NMP domain, therefore its release will tend to be slow and corresponds to the bottleneck step of the enzymatic cycle. Such asymmetric distributions of the frustration at the two binding sites is a prerequisite for the enzyme to be able to
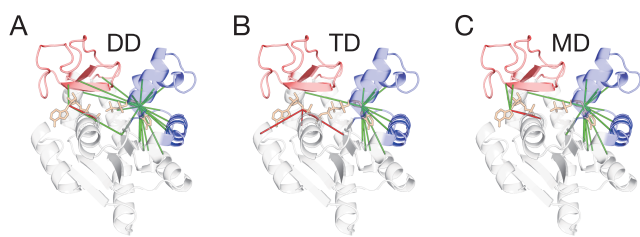
Figure 4. Localized frustration around the ligand binding sites of AdK. (A) Localized frustration pattern of the two product ADP binding sites at the chemical state DD. The protein is shown by cartoon representation. The contacts between the binding residues and the two product ADPs with minimal frustration and high frustration were shown by green lines and red lines, respectively. The two ligands were colored orange. (B, C) Localized frustration pattern of the two ligand binding sites at the chemical states TD (B) and MD (C).

sample the sterically frustrated TD state and therefore is vital to overcome the bottleneck product release step of the enzymatic cycle.[31] As the identities of the two ligands at the binding sites are the same (ADPs), the asymmetry in the energetic frustration of the two sites largely arises from the differences between the two binding sites. Similar results can also be observed for the chemical states with ATP or AMP bound at the LID domain site (Figure 4B,C and Supporting Information, Figure S10). Interestingly, the binding sites at the TD state are relatively more frustrated compared to those at the DD and MD states (Figure 4), which also supports the above discussions that nonspecific AMP binding at the LID domain site tends to reduce the frustration and therefore slows down the product ADP release. We also carried out frustratometer analysis based on the AdK structures from different organisms both for the cases with and without Mg^{2+} (Supporting Information Figures S11, S12, and S13). The above asymmetric distributions of the frustration at the two binding sites was seen for all the investigated structures. Here the frustration index was calculated using the frustratometer based on the contact energies between the ligand and the binding site residues.[36] Therefore, the obtained frustration index corresponds to energetic frustration. The steric

frustration in the chemical state TD arises from the steric incompatibility due to the additional phosphate group.

According to the above discussion, the localized steric frustration at the TD state arising from the additional phosphate group partially disrupts the surrounding residues and destabilizes ADP binding, thereby contributing to the product ADP release. To demonstrate this effect dynamically, we performed short atomistic MD simulations to relax the enzyme starting from the native structure at the chemical states TD, DD, and MD, respectively. We mainly focused on the structural and energetic features of the binding site at the NMP domain, which corresponds to the binding site of the bottleneck product ADP. One can see that at the chemical state DD, the binding site at the NMP domain remain localized around the native structure (Figure 5A). In comparison, the ATP binding at the chemical state TD leads to clear destabilization of the ADP binding site at the NMP domain, as illustrated by the increased RMSD values and total contact energies of the binding site (Figure 5B). Such destabilization of the binding site may facilitate the bottleneck ADP release and the overall catalysis. In comparison, when AMP nonspecifically binds at the LID domain site, which leads to the chemical state MD, the destabilization of the ADP binding site is rather minor (Figure 5C). The different effects of ATP and AMP binding at the LID domain site on the stability of the bottleneck ADP binding site contribute to the observed substrate inhibition when the AMP concentration is high, which is consistent with the kinetic repartitioning mechanism of substrate inhibition discussed above.

Single-Molecule Enzyme Kinetics with Substrate Inhibition. Traditional enzymology studies mostly focus the ensemble level characterization of the enzyme kinetics. With the development of single-molecule techniques, one can measure the turnover rate at the single-molecule level.[53−58] Previous single-molecule studies for another enzyme have shown that the single-molecule turnover time follows a nonexponential distribution.[54] The above dynamic energy landscape model is capable of providing single-molecule level enzyme kinetics. Therefore, it is interesting to investigate how the substrate inhibition is featured by the single-molecule enzyme kinetics. Figure 6 shows the distributions of the single-molecule turnover time, which is defined as the time needed by
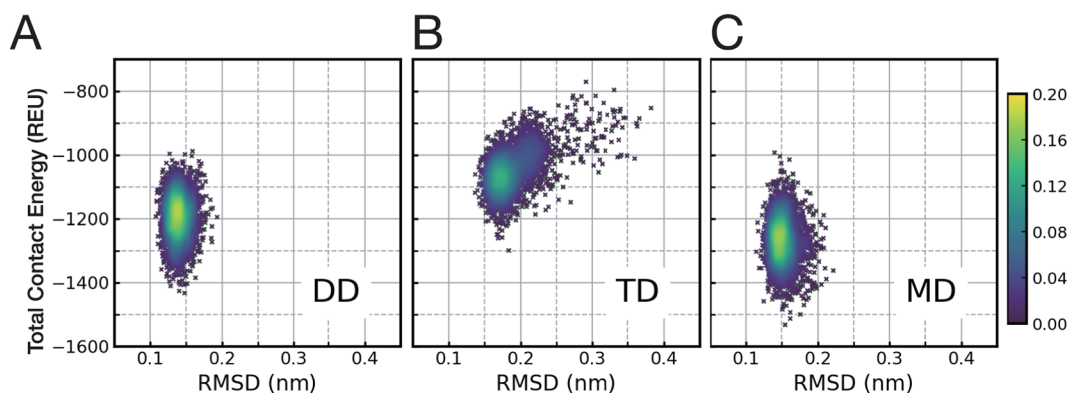
Figure 5. Conformational distribution of the bottleneck product ADP binding site (NMP domain) sampled by short atomistic MD simulations along the reaction coordinates RMSD and contact energy for the chemical states DD (A), TD (B), and MD (C). Here the RMSD measures the root-mean-square deviation of the bottleneck product ADP binding site with respect to the corresponding structure at the native state. The total contact energies correspond to the summation of pairwise contact energies between all the residue pairs at the ADP binding site of the NMP domain. The pairwise contact energies were calculated following ref 36 based on the rosseta energy function.[52] The total contact energies were shown with the rosseta energy unit (REU).
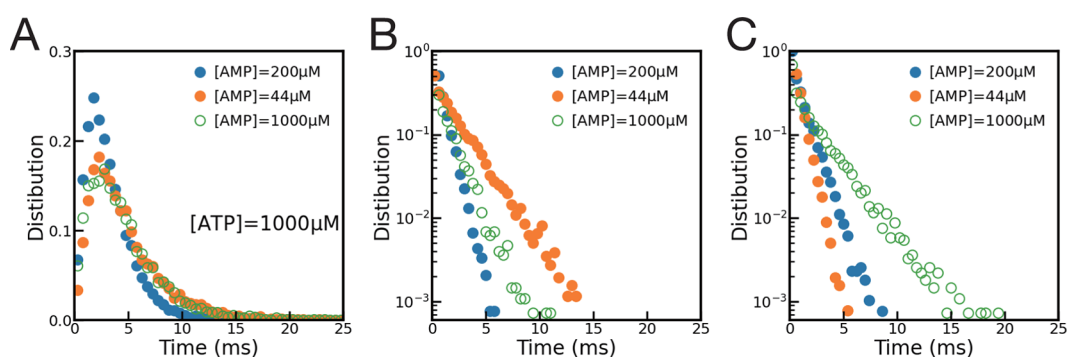
Figure 6. Effect of substrate inhibition on the single-molecule enzymatic kinetics for ATP concentrations of 1000 μM. (A) Distribution of the single-molecule turnover time at different AMP concentrations calculated based on the time interval of the full catalytic-cycle; (B) Distribution of the time interval for sampling the catalytically competent state; (C) Distribution of the time interval for the release of the rate-limiting product ADP.

the enzyme to complete one full catalytic cycle. One can see that the distributions of the catalytic time show nonexponential characteristics, which is in line with previous single-molecule measurements (Figure 6A).[54] As expected, at the AMP concentrations of 1000 μM, at which the substrate inhibition is significant, the population of the events with longer turnover times becomes much higher compared to the case at the optimal substrate concentration (200 μM). Interestingly, although the overall turnover time has an nonexponential distribution, the time intervals for the individual steps of the enzymatic cycle show typical exponential distributions, which may suggest that nonexponential distribution of turnover time typically observed in single-molecule experimental measurements in many cases can arise from the population of long-lived intermediates in the enzymatic cycle. The overall distribution of the turnover time for the simulations with product inhibition ([AMP] = 1000 μM) is similar to that with insufficient substrate ([AMP] = 44 μM) (Figure 6A). However, the time distributions of the individual steps show dramatic differences (Figure 6B,C). At the AMP concentrations of 44 μM, the distribution of the time interval for sampling the catalytically competent state has a wider distribution with elevated distribution of the long time events. In comparison, at the AMP concentrations of 1000 μM with significant substrate inhibition, the distribution of the time interval for the release of the rate-limiting product ADP is much wider. Such results demonstrate the key feature of substrate inhibition at the single-molecule level and support the idea that the substrate inhibition of AdK mainly arises from the product release step.

CONCLUSIONS

Substrate inhibition is one of the most intriguing observations in enzyme catalysis and has relevance both to basic biology and drug development. As an enzymatic cycle involves a tight interplay among many individual physical and chemical steps, unambiguously interpreting the underlying molecular mechanism of substrate inhibition requires a single-molecule level model. In this work, by using a dynamic energy landscape model combined with frustration analysis and all-atom MD simulations, a kinetic repartitioning mechanism of substrate inhibition for the enzyme AdK is revealed. By this mechanism, high concentrations of substrate suppress the population of the energetically frustrated substrate—product cobound complex which features steric incompatibility, that slows down the bottleneck product release and overall catalysis. Such a

mechanism suggests that the substrate inhibition of AdK mainly arises from the slowing of the product release step, instead of the steps involved in the population of the catalytically competent complex, as previously suggested. The substrate inhibition effect is closely correlated with the conformational equilibria of the enzyme. Enzyme mutants with conformational equilibria biased to closed states tend to show stronger substrate inhibition, which is in line with a previous experimental observation that mutations increasing the enzyme stability often have enhanced substrate inhibition effect. We have also characterized the substrate inhibition effect based on the single-molecule enzymatics, which is featured by the wider distribution of the product release time.

In conclusion, this work provides a clear picture using single-molecule level computational simulations of the origin of the substrate inhibition effect of enzyme catalysis. The results reveal a previously unrecognized molecular mechanism of substrate inhibition and establish a link between substrate inhibition, frustration of energy landscape, enzyme conformational equilibrium, and the single-molecule enzyme kinetics.

ASSOCIATED CONTENT

Ⓢ Supporting Information

The Supporting Information is available free of charge at https://pubs.acs.org/doi/10.1021/acs.jpcb.2c03832.

> Details of the computational model, molecular simulations, and some additional results (PDF)

AUTHOR INFORMATION

Corresponding Authors

Wenfei Li − *Department of Physics, National Laboratory of Solid State Microstructure, and Collaborative Innovation Center of Advanced Microstructures, Nanjing University, Nanjing 210093, China; Wenzhou Institute, University of Chinese Academy of Sciences, Wenzhou, Zhejiang 325000, China;* ⓄRCID orcid.org/0000-0003-2679-4075; Email: wfli@nju.edu.cn

Peter G. Wolynes − *Center for Theoretical Biological Physics, Rice University, Houston, Texas 77005, United States;* ⓄRCID orcid.org/0000-0001-7975-9287; Email: pwolynes@rice.edu

Wei Wang − *Department of Physics, National Laboratory of Solid State Microstructure, and Collaborative Innovation Center of Advanced Microstructures, Nanjing University,*

Nanjing 210093, China; ● orcid.org/0000-0001-5441-0302; Email: wangwei@nju.edu.cn

Authors

Yangyang Zhang − *Department of Physics, National Laboratory of Solid State Microstructure, and Collaborative Innovation Center of Advanced Microstructures, Nanjing University, Nanjing 210093, China; Wenzhou Institute, University of Chinese Academy of Sciences, Wenzhou, Zhejiang 325000, China;* ● orcid.org/0000-0001-7449-7740

Mingchen Chen − *Department of Research and Development, neoX Biotech, Beijing 102206, China; Center for Theoretical Biological Physics, Rice University, Houston, Texas 77005, United States;* ● orcid.org/0000-0003-3916-7871

Jiajun Lu − *Department of Physics, National Laboratory of Solid State Microstructure, and Collaborative Innovation Center of Advanced Microstructures, Nanjing University, Nanjing 210093, China*

Complete contact information is available at:
https://pubs.acs.org/10.1021/acs.jpcb.2c03832

Notes

The authors declare no competing financial interest.

■ REFERENCES

(1) Segel, I. H. *Enzyme Kinetics*; Wiley: New York, 1993.

(2) Hill, G. A.; Robinson, C. W. Substrate inhibition kinetics: phenol degradation by Pseudomonas putida. *Biotechnol. Bioeng.* **1975**, *17*, 1599−1615.

(3) Efimov, I.; Basran, J.; Sun, X.; Chauhan, N.; Chapman, S. K.; Mowat, C. G.; Raven, E. L. The mechanism of substrate inhibition in human indoleamine 2, 3-dioxygenase. *J. Am. Chem. Soc.* **2012**, *134*, 3034−3041.

(4) Weber, B.; Nickel, E.; Horn, M.; Nienhaus, K.; Nienhaus, G. U. Substrate inhibition in human indoleamine 2, 3-dioxygenase. *J. Phys. Chem. Lett.* **2014**, *5*, 756−761.

(5) Kojima, T.; Takayama, S. Membraneless compartmentalization facilitates enzymatic cascade reactions and reduces substrate inhibition. *ACS Appl. Mater. Interfaces* **2018**, *10*, 32782−32791.

(6) Szegletes, T.; Mallender, W. D.; Thomas, P. J.; Rosenberry, T. L. Substrate binding to the peripheral site of acetylcholinesterase initiates enzymatic catalysis. Substrate inhibition arises as a secondary effect. *Biochemistry* **1999**, *38*, 122−133.

(7) LiCata, V. J.; Allewell, N. M. Is substrate inhibition a consequence of allostery in aspartate transcarbamylase? *Biophys. Chem.* **1997**, *64*, 225−234.

(8) Lin, Y.; Lu, P.; Tang, C.; Mei, Q.; Sandig, G.; Rodrigues, A. D.; Rushmore, T. H.; Shou, M. Substrate inhibition kinetics for cytochrome P450-catalyzed reactions. *Drug Metab. Dispos.* **2001**, *29*, 368−374.

(9) McEachern, K. A.; Fung, J.; Komarnitsky, S.; Siegel, C. S.; Chuang, W.-L.; Hutto, E.; Shayman, J. A.; Grabowski, G. A.; Aerts, J. M.; Cheng, S. H.; et al. A specific and potent inhibitor of glucosylceramide synthase for substrate inhibition therapy of Gaucher disease. *Mol. Genet. Metab.* **2007**, *91*, 259−267.

(10) Cheng, A.; Zhang, P.; Wang, B.; Yang, D.; Duan, X.; Jiang, Y.; Xu, T.; Jiang, Y.; Shi, J.; Ding, C.; et al. Aurora-A mediated phosphorylation of LDHB promotes glycolysis and tumor progression by relieving the substrate-inhibition effect. *Nat. Commun.* **2019**, *10*, 1−16.

(11) Vesell, E. S. Lactate dehydrogenase isozymes: substrate inhibition in various human tissues. *Science* **1965**, *150*, 1590−1593.

(12) Peng, S.; Van Der Donk, W. A. An unusual isotope effect on substrate inhibition in the oxidation of arachidonic acid by lipoxygenase. *J. Am. Chem. Soc.* **2003**, *125*, 8988−8989.

(13) Liang, P.; Phillips, G. N., Jr; Glaser, M. Assignment of the nucleotide binding sites and the mechanism of substrate inhibition of Escherichia coli adenylate kinase. *Proteins: Struct., Funct., Bioinf.* **1991**, *9*, 28−36.

(14) Furman, P. A.; Painter, G.; Wilson, J. E.; Cheng, N.; Hopkins, S. Substrate inhibition of the human immunodeficiency virus type 1 reverse transcriptase. *Proceedings of the National Academy of Sciences of the USA* **1991**, *88*, 6013−6017.

(15) Reed, M. C.; Lieb, A.; Nijhout, H. F. The biological significance of substrate inhibition: A mechanism with diverse functions. *BioEssays* **2010**, *32*, 422−429.

(16) Adkar, B. V.; Bhattacharyya, S.; Gilson, A. I.; Zhang, W.; Shakhnovich, E. I. Substrate inhibition imposes fitness penalty at high protein stability. *Proceedings of the National Academy of Sciences of the USA* **2019**, *116*, 11265−11274.

(17) Tan, Y.-W.; Hanson, J. A.; Yang, H. Direct Mg2+ binding activates adenylate kinase from Escherichia coli. *J. Biol. Chem.* **2009**, *284*, 3306−3313.

(18) Tronconi, M. A.; Wheeler, M. C. G.; Martinatto, A.; Zubimendi, J. P.; Andreo, C. S.; Drincovich, M. F. Allosteric substrate inhibition of Arabidopsis NAD-dependent malic enzyme 1 is released by fumarate. *Phytochemistry* **2015**, *111*, 37−47.

(19) Brezovsky, J.; Babkova, P.; Degtjarik, O.; Fortova, A.; Gora, A.; Iermak, I.; Rezacova, P.; Dvorak, P.; Smatanova, I. K.; Prokop, Z.; et al. Engineering a de novo transport tunnel. *ACS Catal.* **2016**, *6*, 7597−7610.

(20) Kokkonen, P.; Beier, A.; Mazurenko, S.; Damborsky, J.; Bednar, D.; Prokop, Z. Substrate inhibition by the blockage of product release and its control by tunnel engineering. *RSC Chemical Biology* **2021**, *2*, 645−655.

(21) Müller, C.; Schlauderer, G.; Reinstein, J.; Schulz, G. E. Adenylate Kinase Motions During Catalysis: An Energetic Counterweight Balancing Substrate Binding. *Structure* **1996**, *4*, 147−156.

(22) Henzler-Wildman, K. A.; Thai, V.; Lei, M.; Ott, M.; Wolf-Watz, M.; Fenn, T.; Pozharski, E.; Wilson, M. A.; Petsko, G. A.; Karplus, M.; et al. Intrinsic Motions Along An Enzymatic Reaction Trajectory. *Nature* **2007**, *450*, 838−844.

(23) Hanson, J. A.; Duderstadt, K.; Watkins, L. P.; Bhattacharyya, S.; Brokaw, J.; Chu, J.-W.; Yang, H. Illuminating the Mechanistic Roles of Enzyme Conformational Dynamics. *Proceedings of the National Academy of Sciences of the USA* **2007**, *104*, 18055−18060.

(24) Lu, Q.; Wang, J. Single Molecule Conformational Dynamics of Adenylate Kinase: Energy Landscape, Structural Correlations, and Transition State Ensembles. *J. Am. Chem. Soc.* **2008**, *130*, 4772−4783.

(25) Miyashita, O.; Onuchic, J. N.; Wolynes, P. G. Nonlinear Elasticity, Proteinquakes, and the Energy Landscapes of Functional Transitions in Proteins. *Proceedings of the National Academy of Sciences of the USA* **2003**, *100*, 12570−12575.

(26) Daily, M. D.; Phillips, G. N.; Cui, Q. Many Local Motions Cooperate to Produce the Adenylate Kinase Conformational Transition. *J. Mol. Biol.* **2010**, *400*, 618−631.

(27) Whitford, P. C.; Gosavi, S.; Onuchic, J. N. Conformational Transitions in Adenylate Kinase Allosteric Communication Reduces Misligation. *J. Biol. Chem.* **2008**, *283*, 2042−2048.

(28) Pirchi, M.; Ziv, G.; Riven, I.; Cohen, S. S.; Zohar, N.; Barak, Y.; Haran, G. Single-Molecule Fluorescence Spectroscopy Maps the Folding Landscape of A Large Protein. *Nat. Commun.* **2011**, *2*, 493.

(29) Kovermann, M.; Ådén, J.; Grundström, C.; Sauer-Eriksson, A. E.; Sauer, U. H.; Wolf-Watz, M. Structural Basis for Catalytically Restrictive Dynamics of A High-Energy Enzyme State. *Nat. Commun.* **2015**, *6*, 7644.

(30) Pisliakov, A. V.; Cao, J.; Kamerlin, S. C.; Warshel, A. Enzyme Millisecond Conformational Dynamics Do Not Catalyze the Chemical Step. *Proceedings of the National Academy of Sciences of the USA* **2009**, *106*, 17359−17364.

(31) Li, W.; Wang, J.; Zhang, J.; Takada, S.; Wang, W. Overcoming the Bottleneck of the Enzymatic Cycle by Steric Frustration. *Phys. Rev. Lett.* **2019**, *122*, 238102.

(32) Aviram, H. Y.; Pirchi, M.; Mazal, H.; Barak, Y.; Riven, I.; Haran, G. Direct observation of ultrafast large-scale dynamics of an enzyme under turnover conditions. *Proceedings of the National Academy of Sciences of the USA* **2018**, *115*, 3243−3248.

(33) Pelz, B.; Žoldák, G.; Zeller, F.; Zacharias, M.; Rief, M. Subnanometre enzyme mechanics probed by single-molecule force spectroscopy. *Nat. Commun.* **2016**, *7*, 1−9.

(34) Kong, J.; Li, J.; Lu, J.; Li, W.; Wang, W. Role of substrate-product frustration on enzyme functional dynamics. *Phys. Rev. E* **2019**, *100*, 052409.

(35) Sinev, M. A.; Sineva, E. V.; Ittah, V.; Haas, E. Towards a mechanism of AMP-substrate inhibition in adenylate kinase from Escherichia coli. *FEBS letters* **1996**, *397*, 273−276.

(36) Chen, M.; Chen, X.; Schafer, N. P.; Clementi, C.; Komives, E. A.; Ferreiro, D. U.; Wolynes, P. G. Surveying biomolecular frustration at atomic resolution. *Nat. Commun.* **2020**, *11*, 1−9.

(37) Clementi, C.; Nymeyer, H.; Onuchic, J. N. Topological and energetic factors: what determines the structural details of the transition state ensemble and "en-route" intermediates for protein folding? An investigation for small globular proteins. *J. Mol. Biol.* **2000**, *298*, 937−953.

(38) Onuchic, J. N.; Luthey-Schulten, Z.; Wolynes, P. G. Theory of protein folding: the energy landscape perspective. *Annu. Rev. Phys. Chem.* **1997**, *48*, 545−600.

(39) Okazaki, K. I.; Koga, N.; Takada, S.; Onuchic, J. N.; Wolynes, P. G. Multiple-basin energy landscapes for large-amplitude conformational motions of proteins: Structure-based molecular dynamics simulations. *Proceedings of the National Academy of Sciences of the USA* **2006**, *103*, 11844−11849.

(40) Okazaki, K.-I.; Takada, S. Dynamic energy landscape view of coupled binding and protein conformational change: Induced-fit versus population-shift mechanisms. *Proceedings of the National Academy of Sciences of the USA* **2008**, *105*, 11182−11187.

(41) Kenzaki, H.; Koga, N.; Hori, N.; Kanada, R.; Li, W.; Okazaki, K.-I.; Yao, X.-Q.; Takada, S. CafeMol: A coarse-grained biomolecular simulator for simulating proteins at work. *J. Chem. Theory Comput.* **2011**, *7*, 1979−1989.

(42) Müller, C. W.; Schulz, G. E. Structure of the complex between adenylate kinase from Escherichia coli and the inhibitor Ap5A refined at 1.9 Å resolution: A model for a catalytic transition state. *J. Mol. Biol.* **1992**, *224*, 159−177.

(43) Abraham, M. J.; Murtola, T.; Schulz, R.; Pall, S.; Smith, J. C.; Hess, B.; Lindahl, E. GROMACS: High performance molecular simulations through multi-level parallelism from laptops to super-computers. *SoftwareX* **2015**, *1−2*, 19−25.

(44) Hornak, V.; Abel, R.; Okur, A.; Strockbine, B.; Roitberg, A.; Simmerling, C. Comparison of multiple Amber force fields and development of improved protein backbone parameters. *Proteins: Struct., Funct., Bioinf.* **2006**, *65*, 712−725.

(45) Jorgensen, W. L.; Chandrasekhar, J.; Madura, J. D.; Impey, R. W.; Klein, M. L. Comparison of simple potential functions for simulating liquid water. *J. Chem. Phys.* **1983**, *79*, 926−935.

(46) Ådén, J.; Verma, A.; Schug, A.; Wolf-Watz, M. Modulation of a pre-existing conformational equilibrium tunes adenylate kinase activity. *J. Am. Chem. Soc.* **2012**, *134*, 16562−16570.

(47) Kovermann, M.; Grundström, C.; Sauer-Eriksson, A. E.; Sauer, U. H.; Wolf-Watz, M. Structural basis for ligand binding to an enzyme by a conformational selection pathway. *Proc. Natl. Acad. Sci. U. S. A.* **2017**, *114*, 6298−6303.

(48) Ådén, J.; Wolf-Watz, M. NMR Identification of Transient Complexes Critical to Adenylate Kinase Catalysis. *J. Am. Chem. Soc.* **2007**, *129*, 14003−14012.

(49) Ferreiro, D. U.; Komives, E. A.; Wolynes, P. G. Frustration in biomolecules. *Q. Rev. Biophys.* **2014**, *47*, 285−363.

(50) Li, W.; Wolynes, P. G.; Takada, S. Frustration, specific sequence dependence, and nonlinearity in large-amplitude fluctuations of allosteric proteins. *Proceedings of the National Academy of Sciences of the USA* **2011**, *108*, 3504−3509.

(51) Ferreiro, D. U.; Hegler, J. A.; Komives, E. A.; Wolynes, P. G. On the role of frustration in the energy landscapes of allosteric proteins. *Proc. Natl. Acad. Sci. U. S. A.* **2011**, *108*, 3499−3503.

(52) Alford, R. F.; et al. The Rosetta All-Atom Energy Function for Macromolecular Modeling and Design. *J. Chem. Theory Comput.* **2017**, *13*, 3031−3048.

(53) Xie, X. S. Enzyme kinetics, past and present. *Science* **2013**, *342*, 1457−1459.

(54) English, B. P.; Min, W.; Van Oijen, A. M.; Lee, K. T.; Luo, G.; Sun, H.; Cherayil, B. J.; Kou, S.; Xie, X. S. Ever-Fluctuating Single Enzyme Molecules: Michaelis-Menten Equation Revisited. *Nat. Chem. Biol.* **2006**, *2*, 87−94.

(55) Lu, H. P.; Xun, L.; Xie, X. S. Single-Molecule Enzymatic Dynamics. *Science* **1998**, *282*, 1877−1882.

(56) Min, W.; Luo, G.; Cherayil, B. J.; Kou, S.; Xie, X. S. Observation of A Power-Law Memory Kernel for Fluctuations Within A Single Protein Molecule. *Phys. Rev. Lett.* **2005**, *94*, 198302.

(57) Gershenson, A. Single molecule enzymology: Watching the reaction. *Curr. Opin. Chem. Biol.* **2009**, *13*, 436−442.

(58) Wang, J.; Wolynes, P. Intermittency of single molecule reaction dynamics in fluctuating environments. *Phys. Rev. Lett.* **1995**, *74*, 4317.